

Ramsey pulse optimization for atomic fountains

V. S. Tavares^{1,2}, L. V. G. Tarelho², D. V. Magalhães¹

¹ National Institute of Metrology, Quality, and Technology, Duque de Caxias, Rio de Janeiro, 25250-020, Brazil

² University of São Paulo, São Carlos, SP, Brazil

ABSTRACT

Atomic frequency standards realize the measurement of the atomic transition frequency between two well-defined quantum energy levels. This study uses the Euler–Cromer method to numerically analyse the atomic transition probabilities for the caesium fountain clock, based on the Ramsey method of separate fields. Consequently, this examination successfully attains an optimal compromise correlation among the oscillating field (B_0), static field (B_z), and detuning (δw). Thus, this work presents a new tool for time and frequency metrology standardization.

Section: RESEARCH PAPER

Keywords: Rabi oscillations; Ramsey pulse; two-level system; caesium fountain clocks; time and frequency metrology

Citation: V. S. Tavares, L. V. G. Tarelho, D. V. Magalhães, Ramsey pulse optimization for atomic fountains, Acta IMEKO, vol. 15 (2026) no. 1, pp. 1-5. DOI: [10.21014/actaimeko.v15i1.1975](https://doi.org/10.21014/actaimeko.v15i1.1975)

Section Editor: Carlos Hall, PósMQI/PUC-Rio, Rio de Janeiro, Brazil

Received November 10, 2024; **In final form** December 8, 2025; **Published** March 2026

Copyright: This is an open-access article distributed under the terms of the [Creative Commons Attribution 4.0 International License](https://creativecommons.org/licenses/by/4.0/).

Funding: This work was supported by the Brazilian funding agencies CNPq, FINEP, FAPESP, and CAPES (Coordenação de Aperfeiçoamento de Pessoal de Nível Superior) – Brazil – Finance.

Corresponding author: Vitor Silva Tavares, e-mail: vitorstum@gmail.com

1. INTRODUCTION

Understanding a two-level quantum system is vital in many areas, such as quantum computation [1], quantum metrology [2], quantum sensing [3], and quantum frequency standardization [4]. For this last application, caesium fountain clocks serve as reference to the international atomic time scale TAI [5]. The operating mode of caesium atomic clocks uses the microwave cavity to induce atomic transitions between hyperfine two-level states of the caesium atom. This type of caesium clock presents exceptional levels of uncertainty measurement with stability on the order of $10^{-15} \tau^{-1/2}$ and an accuracy estimated for a relative uncertainty of 10^{-16} .

The operation of the caesium fountain clock is based on Rabi oscillations [6] and the Ramsey method [7], in which an atomic cloud is interrogated twice through a resonator (microwave cavity), generating the atomic transition. The Rabi and Ramsey signals are fundamental for performing a caesium fountain clock. Many factors can affect the atomic transition in this type of clock, like gravitational effects [8], AC Stark effect [9], Zeeman effect [10], black body radiation [11], and others. All these effects degrade the signal, causing undesirable frequency shifts.

In particular, in an atomic caesium fountain clock, a static magnetic field, named C-field, is applied to the region from below the microwave cavity to the highest point the atoms reach

to perform the Ramsey method during the time of flight of the atoms. The interaction of the atoms with the C-field is used to provide a quantization axis to separate the field-dependent transitions from the clock transition $6^2S_{1/2} |F = 3, m_f = 0\rangle \rightarrow 6^2P_{1/2} |F = 4, m_f = 0\rangle$, to avoid overlapping lines as much as possible [10]. However, the C-field induces a significant frequency shift of the measured hyperfine levels of the atoms, which needs to be corrected for better clock performance. In the scientific literature, this frequency shift is known as a Second-Order Zeeman Shift (SOZS) [10], [12], [13]. One way to estimate the SOZS is to obtain averaged C-field values from Zeeman frequency data for several launching heights of the atomic cloud [14], [15].

In this context, the present work proposes a numerical solution based on the Euler–Cromer method for studied Ramsey pulses used in the clock of the atomic caesium fountain. Using this new computational tool, an optimization can be made for the value of the oscillating field coming from the microwave cavity, the C-field for all interaction regions of the atoms, and an estimation for the detuning value is performed. Our goal is to evaluate the impact of the C-field on the atoms, obtaining a suitable time interval that minimizes the detuning. Therefore, this work aims to contribute to both the application fields of quantum metrology and time and frequency metrology.

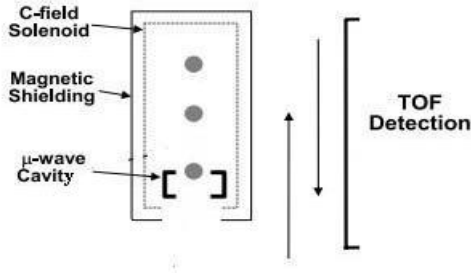


Figure 1. A schematic diagram of the caesium fountain clock.

2. BASIC PRINCIPLE

2.1 Theoretical model

The atomic transition between two hyperfine levels of the states $6^2S_{1/2} |F = 3, m_f = 0\rangle \rightarrow 6^2P_{1/2} |F = 4, m_f = 0\rangle$ reproduces the primary definition for the second, according to the new SI. To excite an atomic transition between these levels in the caesium fountain clock, the Ramsey interrogation method [7] is used, in which the atoms undergo two oscillatory perturbations separated by a perturbation-free region. The atoms interact with the C-field throughout the process, causing the frequency shift. As the magnetic induction separates each of the seven transitions $\Delta F = \pm 1.0$ and $\Delta m_f = 0$ of their neighbourhoods, approximating a two-level system interacting with magnetic fields is valid. A basic schematic diagram of the caesium fountain is shown in Figure 1.

As can be seen in Figure 1, the flight tower consists of a microwave cavity for interrogating the atomic cloud, a solenoid to produce the C-field, and a magnetic shield to prevent perturbations from stray magnetic fields. A cylinder of μ -metal is placed around the free-flight tower [16]. For weak static and oscillating field values, it is possible to describe all the interactions experienced by the atomic cloud by:

$$i \hbar \dot{C}_3 = \frac{g_j \mu_b B_Z}{2} C_3 + \frac{g_j \mu_b B_0}{2} e^{-i \delta \omega t} C_4, \quad (1)$$

$$\hbar \dot{C}_4 = -\frac{g_j \mu_b B_Z}{2} C_4 + \frac{g_j \mu_b B_0}{2} e^{i \delta \omega t} C_3, \quad (2)$$

where \hbar is the reduced Planck constant; g_j is the gyromagnetic factor of the electron; μ_b is the Bohr magneton; B_Z and B_0 are the static and oscillating magnetic fields, respectively, and $\delta \omega$ is the detuning between the frequency atomic transition and microwave frequency. C_3 and C_4 are the probability amplitudes of the hyperfine levels F_3 and F_4 , respectively [17], [18]. One can rewrite equation 1 and 2 as:

$$i \dot{C}_3 = \frac{\gamma}{2} C_3 + \frac{b}{2} e^{-i \delta \omega t} C_4, \quad (3)$$

$$i \dot{C}_4 = -\frac{\gamma}{2} C_4 + \frac{b}{2} e^{i \delta \omega t} C_3, \quad (4)$$

where $\gamma = g_j \mu_b B_Z / \hbar$ is the Larmor frequency and $b = g_j \mu_b B_0 / \hbar$ is the Rabi frequency.

2.2 Numerical solution

On this point, we describe the method for calculating the transition probability between the two levels, assuming the approach to calculate a single atomic transition probability [19].

Thus, applying these assumptions, the Euler–Cromer method is used to solve the coupled differential equations (3) and (4) [20], which can be written as:

$$C_{3j+1} = -i \left[\frac{\gamma}{2} C_{3j+1} + \frac{b}{2} e^{-i \delta \omega t} C_{4j+1} \right] (t_{j+1} - t_j) + C_{3j}, \quad (5)$$

$$C_{4j+1} = -i \left[-\frac{\gamma}{2} C_{4j+1} + \frac{b}{2} e^{i \delta \omega t} C_{3j+1} \right] (t_{j+1} - t_j) + C_{4j}. \quad (6)$$

The programming language used in this study was the Python language. The sequence of coding the numerical solution using the Euler–Cromer method was given as follows: a) importing the libraries; b) defining the known parameters, with $\delta \omega$, B_Z , and B_0 ; c) defining the initial conditions, namely $C_3 = 0 - 0j$, $C_4 = 1.0 + 0j$, and $t_j = 0$; d) defining the time step $dt = t_j + 1.0 - t_j = 1.0 \mu s$; e) implementing the Euler–Cromer method; f) to preserve the probability of transition between the two levels of interest, a normalization is applied so that the sum of the probability amplitudes ($|C_3|^2 + |C_4|^2$) equals 1, followed by the plotting of graphs for analysis. The coding of the Euler method was performed by repeating the following steps:

- 1) Optimization of the oscillating field B_0 – The oscillating magnetic field B_0 was characterized by $B_Z = 0$ and by detuning $\delta \omega = 0$. It evaluated typical values of the B_0 used in the caesium fountain, on the order of nanotesla. At this point, the condition $\tau = \pi/2$ was inserted, where τ is the interaction time between the B_0 and the atomic cloud. In addition, TOF was kept fixed at 20.0 ms.
- 2) Insertion and characterization of the static field B_Z – We characterize the static magnetic field embedded in the entire trajectory of the atoms to realize the Ramsey method.
- 3) Insertion of the detuning $\delta \omega$ – The detuning $\delta \omega$ was inserted to compensate for the effect caused by the C-field again to achieve the maximum transition probability between hyperfine levels. However, to recover the $\pi/2$ pulse in the two passes through the microwave cavity, a variation was made in the amplitude of the oscillatory field to maximize the transition probability in the Ramsey method.

It is important to mention that the atomic cloud was considered as a single atom in this numerical simulation. In addition, the $\pi/2$ pulse is defined here as the pulse in which the transition probability reaches 50 %.

3. RESULTS AND DISCUSSION

The impact of the different oscillating magnetic field B_0 , static magnetic field B_Z , and detuning $\delta \omega$ for a TOF of 20.0 ms is evaluated through the Euler–Cromer method. The first result of this study is a graph of the behaviour of the transition probability amplitudes as a function of the total time of the Ramsey process, in which the oscillating magnetic field is characterized (as shown in Figure 2).

As shown in Figure 2, three typical values of B_0 used in a caesium fountain clock were applied, revealing a reduction in the effective period of the $\pi/2$ pulse. From this first analysis, the value of the oscillating field was fixed at 1.0 nT (Figure 2b), corresponding to the value of $\tau = 8.92$ ms. The next step is inserting the B_Z with an oscillating magnetic field fixed at 1.0 nT. Thus, we now have the spin precession phenomenon, generated by the action of this field, characterized by the Larmor frequency

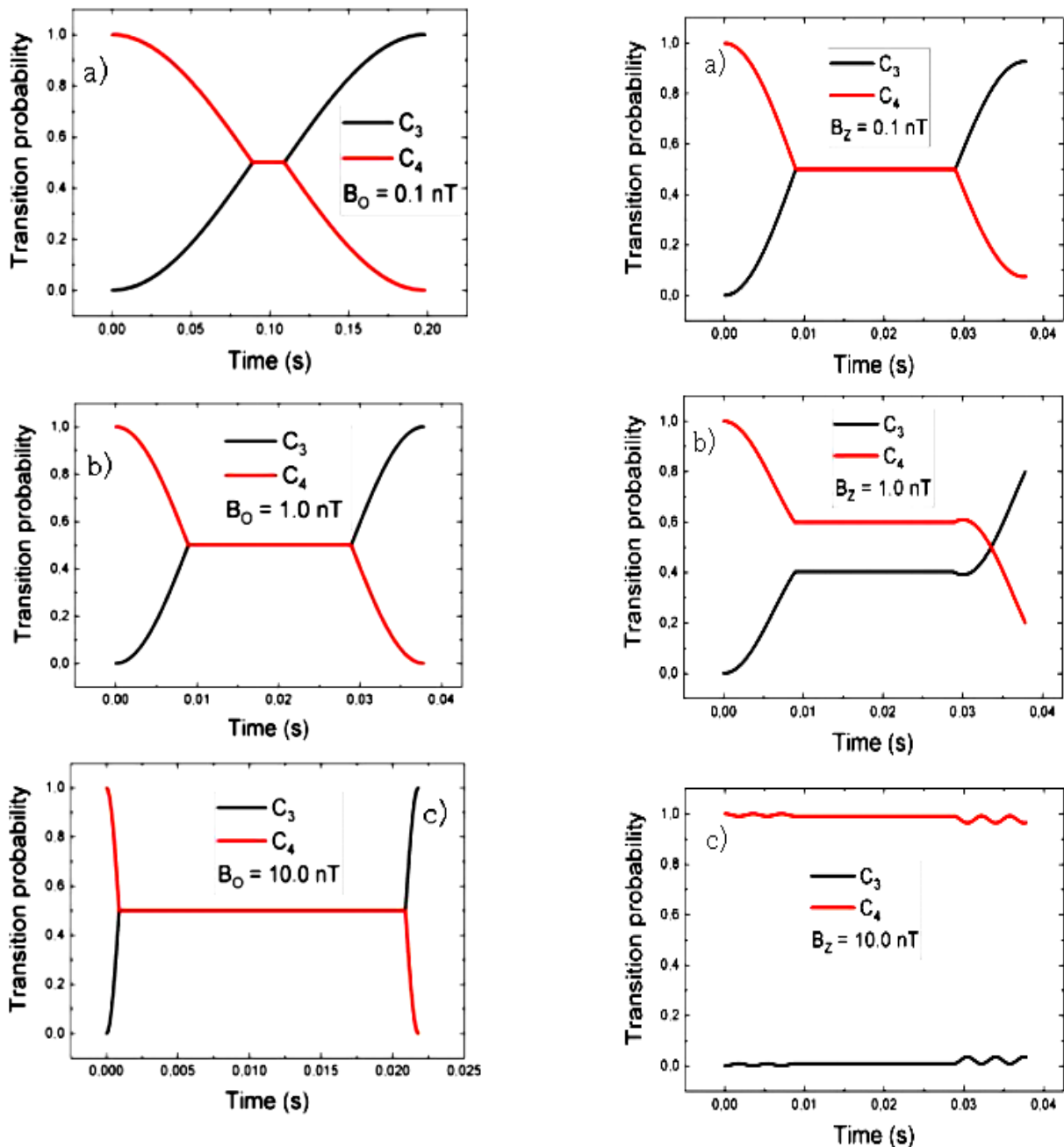


Figure 2. Transition probability amplitudes as a function of the total time of the Ramsey process to different oscillating magnetic fields B_0 .

[17]. Figure 3 shows the effect of the static field on the transition probability between levels.

Figure 3 shows values that were used for characterizing the B_z . It can be seen in Figure 3a that there is no more significant change in the transition amplitude on the first $\pi/2$ pulse. Figure 3b shows that the value of a static field of 1.0 nT is sufficient to generate the desired quantization on the axis of the atoms with field action, impairing the transition probability between the two $\pi/2$ pulses. Furthermore, it can be seen in Figure 3c and Figure 3d that for a static field value of the order of 10.0 nT and 100.0 nT, the transition probability is drastically reduced, and the transition between energy levels does not occur.

In a caesium fountain-type clock, typical C-field values are on the order of hundreds of nanotesla [10]. Thus, the value of the B_z was fixed at 100.0 nT, and a detuning $\delta\omega$ was inserted, in addition to increasing the amplitude of the oscillating field B_0 ,

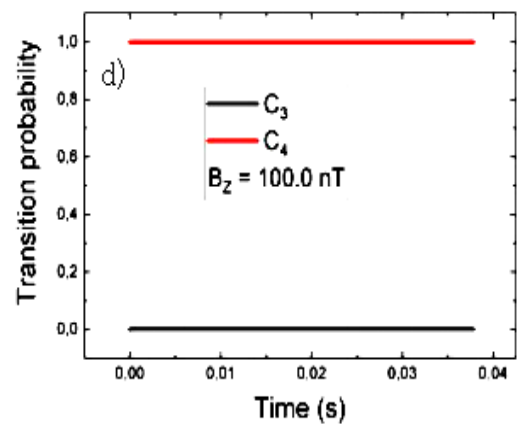


Figure 3. Transition probability amplitudes as a function of the total time of the Ramsey process to characterization static magnetic fields B_z .

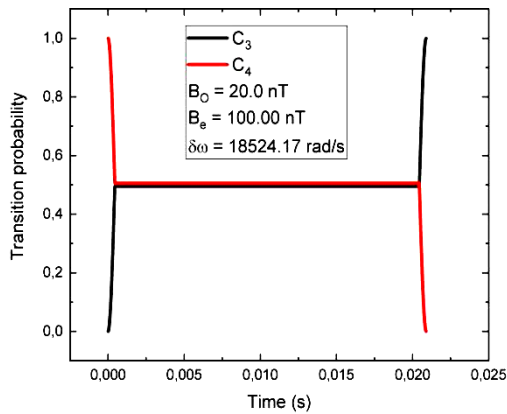


Figure 4. Amplitudes of transition probability as a function of total time of the Ramsey process to optimization of the parameters B_0 , B_z and $\delta\omega$.

focusing on recovering the two $\pi/2$ pulses, as can be seen in Figure 4. It expresses a compromise relation between the parameters varied to obtain the two $\pi/2$ pulses in the caesium fountain. Thus, by changing the value of the oscillating field, its interaction time with the atoms was reduced to $\tau = 0.44$ ms.

The final step was implemented using an expression for the oscillating magnetic field with an x spatial component:

$$B_0 = A \cdot e^{x^2}, \quad (7)$$

where A represents the amplitude of the field, x represents the distance between the origin of the oscillating field and the position of the atomic cloud when it receives the $\pi/2$ pulse. The value of x set at this stage of the simulation was 0.10 m.

In this final stage, the same steps as those previously performed were carried out; however, a new trade-off relation was established to achieve the two $\pi/2$ pulses in a caesium fountain. Thus, the new trade-off relation obtained is $B_0 = 21.5 \times 10^{-9}$ nT, $B_z = 100.00$ nT, $\delta\omega = 20,370.55$ rad/s, which is equivalent to 3,243.71 Hz, with the interaction time with the atoms remaining at $\tau = 0.44$ ms. Through this simulation, the new oscillating magnetic field was obtained, given by:

$$B_0 = 21.5 \cdot e^{x^2}. \quad (8)$$

4. CONCLUSIONS

The present work evaluates the impact of the static field insertion in a caesium fountain-type clock employing a numerical solution of the Rabi oscillations. The numerical method used in this study is the Euler–Cromer method. Focusing on evaluating was achieved by varying the input parameters: oscillating magnetic field B_0 , static magnetic field B_z , and detuning $\delta\omega$. From the analysis carried out, it was possible to obtain two compromise relationships for the input parameters. In the first, we have $B_0 = 20.0$ nT, $B_z = 100.0$ nT, and $\delta\omega = 18,524.17$ rad/s correspondent to $\delta f = 2,949.70$ Hz. In addition, the interaction time of the atoms with the oscillating field was estimated through numerical simulation to be around 0.44 ms, for a value of $TOF = 20.0$ ms.

In the second step, a spatial component for the oscillating magnetic field was considered, following equation (5). It was observed that, for a given distance between the origin of the oscillating magnetic field and the position where the atomic

cloud receives the $\pi/2$ pulse, the amplitude of the oscillating magnetic field shifts to 21.5 nT and the frequency detuning changes to $\delta\omega = 20,370.55$ rad/s, corresponding to $\delta f = 3,243.71$ Hz.

Future work includes the consideration of the temporal part of the oscillating magnetic field and modelling the case of a large number of atoms (of the order of 10^8) for the atomic cloud.

AUTHORS' CONTRIBUTION

Conceived and designed the analysis: Vitor S. Tavares, L. V. G. Tarelho, D. V. Magalhães.

Performed the analysis: Vitor S. Tavares, L. V. G. Tarelho, D. V. Magalhães.

Wrote the paper: Vitor S. Tavares.

ACKNOWLEDGEMENT

Authors acknowledge the financial support provided by the Brazilian funding agencies CNPq, FINEP, FAPESP, and CAPES (Coordenação de Aperfeiçoamento de Pessoal de Nível Superior) – Brazil – Finance.

REFERENCES

- [1] C. A. Muschik, H. Krauter, K. Hammerer, E. Polzik, Quantum information at the interface of light with atomic ensembles and micromechanical oscillators, *Quantum Information Processing* 10 (2011), pp. 839-863. DOI: [10.1007/s11128-011-0294-2](https://doi.org/10.1007/s11128-011-0294-2)
- [2] W. Nawrocki, *Introduction to quantum metrology: quantum standards and instrumentation*, Springer, Heidelberg, 2015, ISBN 978-3-662-45211-5. DOI: [10.1007/978-3-030-19677-6](https://doi.org/10.1007/978-3-030-19677-6)
- [3] C. L. Degen, F. Reinhard, P. Cappellaro, Quantum sensing, *Reviews of Modern Physics* 89 (2017) 3, art. No. 035002. DOI: [10.1103/RevModPhys.89.035002](https://doi.org/10.1103/RevModPhys.89.035002)
- [4] B. L. Schmittberger, D. R. Scherer, A review of contemporary atomic frequency standards, arXiv preprint arXiv:2004.09987, (2020). Online [Accessed 17 January 2026] <https://arxiv.org/abs/2004.09987>
- [5] H. Hachisu, G. Petit, T. Ido, Absolute frequency measurement with uncertainty below 1×10^{-15} using International Atomic Time, *Applied Physics B* 123 (2017), art. No. 34. DOI: [10.1007/s00340-016-6603-9](https://doi.org/10.1007/s00340-016-6603-9)
- [6] S. Ashhab, J. R. Johansson, F. Nori, Rabi oscillations in a qubit coupled to a quantum two-level system, *New Journal of Physics* 8 (2006) 6, art. No. 103. DOI: [10.1088/1367-2630/8/6/103](https://doi.org/10.1088/1367-2630/8/6/103)
- [7] J. Vanier, C. Tomescu, *The quantum physics of atomic frequency standards: recent developments*, CRC Press, 2015, ISBN 9781032565798.
- [8] D. Calonico, A. Cina, I. Bendea, F. Levi, L. Lorini, A. Godone, Gravitational redshift at INRIM, *Metrologia* 44 (2007) 5, L44. DOI: [10.1088/0026-1394/44/5/N03](https://doi.org/10.1088/0026-1394/44/5/N03)
- [9] R. L. Tjoelker, D. G. Enzer, W. M. Klipstein, Light shift measurements in a cesium fountain without the use of mechanical shutters, *Proc. of the IEEE International Frequency Control Symposium and Precise Time Interval (PTTI) Systems and Applications Meeting 2005, Vancouver, Canada, 29-31 August 2005*, p. 6. DOI: [10.1109/FREQ.2005.1573943](https://doi.org/10.1109/FREQ.2005.1573943)
- [10] X. Wang, J. Ruan, D. Liu, Y. Guan, J. Shi, H. Zhang, R. Lin, J. Chen, F. Yu, T. Liu, S. Zhang, The study of second-order Zeeman shift of the cesium fountain clock NTSC-F1, *Proc. of the 2016 IEEE International Frequency Control Symposium (IFCS), IEEE, New Orleans, USA, 09-12 May 2016*, pp. 1-3. DOI: [10.1109/IFCS.2016.7546817](https://doi.org/10.1109/IFCS.2016.7546817)

- [11] J. Han, Y. Zuo, J. Zhang, L. Wang, Theoretical investigation of the black-body Zeeman shift for microwave atomic clocks, *The European Physical Journal D* 73 (2019), pp. 1-5.
DOI: [10.1140/epjd/e2018-90342-1](https://doi.org/10.1140/epjd/e2018-90342-1)
- [12] J.-R. Shi, X. Wang, Y. Bai, F. Yang, Y. Guan, D. Liu, J. Ruan, S. Zhang, Evaluation of second-order Zeeman frequency shift in NTSC-F2, *Chinese Physics B* 30 (2021) 7, art. No. 070601.
DOI: [10.1088/1674-1056/abe375](https://doi.org/10.1088/1674-1056/abe375)
- [13] Y.-H. Park, S. Park, S. Lee, M. Heo, T. Kwon, H. Hong, S. Lee, Inverse problem approach to evaluate quadratic Zeeman effect for an atomic fountain frequency standard KRISS-F1, *Japanese Journal of Applied Physics* 60 (2021) 6, art. No. 062001.
DOI: [10.35848/1347-4065/abf94b](https://doi.org/10.35848/1347-4065/abf94b)
- [14] N.-F. Liu, F. Fang, C. Liang, L. Wei, W. Ping, L. Kun, S. Rui, L. Chu, Accuracy evaluation of NIM5 Cesium fountain clock, *Chinese Physics Letters* 30 (2013) 1, art. No. 010601.
DOI: [10.1088/0256-307X/30/1/010601](https://doi.org/10.1088/0256-307X/30/1/010601)
- [15] F. Fang, M. Li, P. Lin, W. Chen, N. Liu, Y. Lin, P. Wang, K. Liu, R. Suo, T. Li, NIM5 Cs fountain clock and its evaluation, *Metrologia* 52 (2015) 4, pp. 454-460.
DOI: [10.1088/0026-1394/52/4/454](https://doi.org/10.1088/0026-1394/52/4/454)
- [16] M. Ahmed, D. Magalhães, A. Bebechibuli, S. Muller, R. Alves, T. Ortega, J. Weiner, V. Bagnato, The Brazilian time and frequency atomic standards program, *Anais da Academia Brasileira de Ciências* 80 (2008), pp. 217-252.
DOI: [10.1590/S0001-37652008000200002](https://doi.org/10.1590/S0001-37652008000200002)
- [17] S. H. Autler, C. H. Townes, Stark effect in rapidly varying fields, *Physical Review* 100 (1955) 2, pp. 703-716.
DOI: [10.1103/PhysRev.100.703](https://doi.org/10.1103/PhysRev.100.703)
- [18] I. I. Rabi, Space quantization in a gyrating magnetic field, *Physical Review* 51 (1937) 8, pp. 652-658.
DOI: [10.1103/PhysRev.51.652](https://doi.org/10.1103/PhysRev.51.652)
- [19] P. Wolf, S. Bize, A. Clairon, A. Landragin, P. Laurent, P. Lemonde, C. Bordé, Recoil effects in microwave atomic frequency standards: Preliminary results, *Proc. of the 2001 IEEE International Frequency Control Symposium and PDA Exhibition*, IEEE, Seattle, WA, USA, 08 June 2001, pp. 37-45.
DOI: [10.1109/FREQ.2001.956157](https://doi.org/10.1109/FREQ.2001.956157)
- [20] N. M. Janah, F. Falah, Ratnawati, Ishafit, W. Dwandaru, Comparison of Euler and Euler-Cromer Numerical Methods for Undamped and Damped Spring Oscillation, *Indonesian Review of Physics* 4 (2021) 2, pp. 46-54. Online [Accessed 17 January 2026].
<https://distantreader.org/stacks/journals/irip/irip-4803.pdf>